Inorg. Chem. **2006**, *45*, 3782–3788

Solid State Molecular Structures of Transition Metal Hexafluorides

Thomas Drews, Joanna Supeł, Adelheid Hagenbach, and Konrad Seppelt*

Institut für Chemie der Freien Universität, D-14195 Berlin, Germany

Received November 24, 2005

Single-crystal structure determinations of all nine transition metal hexafluorides (Mo, Tc, Ru, Rh, W, Re, Os, Ir, and Pt) at −140 °C are presented. All compounds crystallize alike and have the same molecular structure. The bond length sequence $r_{W-F} \cong r_{Re-F} \cong r_{Os-F} < r_{Ir-F} < r_{Pt-F}$ is confirmed and paralleled by the sequence $r_{Mo-F} \cong r_{Tc-F} \cong r_{Ru-F} < r_{Rh-F}$. Within the limits of precision, no systematic deviation from octahedral symmetry can be established. DFT and ab initio calculations predict octahedral structures for MoF_6 and RhF_6 and tetragonally distorted structures for ReF_6 and RuF_6. The energy barrier toward octahedral structures is only 2.5 kJ mol^{-1} in the two latter cases. Calculated electron affinities are in the sequence $MoF_6 < TcF_6 < RhF_6 < RuF_6$ with a value of 6.98 eV for the latter. $O_2^+RhF_6^-$ crystallized in an undisordered manner in $P\bar{1}$, isostructural to the low-temperature form of $O_2^+AuF_6^-$. RhF_6^- has a D_{4h} compressed octahedral structure, while AuF_6^- is essentially octahedral. The absorption spectrum of TcF_6 and the ^{19}F and ^{195}NMR spectra of PtF_6 are presented.

Introduction

Sixteen molecular hexafluorides are known: main group, transition metals, and actinide hexafluorides. The nine transition metal hexafluorides form the largest and most fascinating group: MoF_6, TcF_6, RuF_6, RhF_6, WF_6, ReF_6, OsF_6, IrF_6, and PtF_6. Many of the physical properties of these nine compounds are very similar. The chemical properties, however, vary strongly. They range from very stable (WF_6) to highly unstable (RhF_6) and from mildly oxidative (WF_6) to extremely oxidative (RuF_6, RhF_6, PtF_6). From a structural viewpoint, these compounds are remarkable. They all seem to have octahedral structures, although they have different electronic states. The d^0 compounds, MoF_6 and WF_6, have always been assumed to be strictly octahedral, until it was discovered, very recently, that the intramolecular ligand exchange (trigonal twist) has a barrier of only 10 (MoF_6) to 15 kcal mol^{-1} (WF_6).[1] But for the other d^1-d^4 hexafluorides, this barrier is expected to increase.[1] For some of those, however, there is the problem of *Jahn−Teller* distortion. This distortion is expected to be small, and certain peculiarities in the vibrational spectra have been interpreted in terms of a *Jahn−Teller* effect as early as 1959.[2,3]

Recently, the gas-phase molecular structures of WF_6, ReF_6, OsF_6, IrF_6, and PtF_6 have been remeasured by electron diffraction with the utmost possible precision.[4] Deviations from octahedral symmetry are such that, if they exist at all, they are too small to be established with certainty. Ab initio and density functional calculations[4,5] give an indication of the reason for this: ReF_6, OsF_6, IrF_6, and PtF_6 are calculated to have D_{4h} (elongated or compressed octahedral) structures, but the energy difference from the regular octahedral structure is so small (a few kJ mol^{-1}) that rapid interconversion should occur.

These calculations have been performed without considering spin−orbit coupling. This has been justified until now because spin−orbit coupling has been considered to have no structural effects on ground states normally. A strong effect on the structure has been established only occasionally (e.g., for the species CH_2ClI^+).[6] One might speculate that inclusion of spin−orbit coupling in the calculations could indeed drive some of the hexafluorides from distorted to regular octahedral. The energy splitting by spin−orbit coupling for third-row transition metals is a good fraction of the very large ligand-field splitting in these octahedral species. For the second transition metal series, the spin-orbit

* To whom correspondence should be addressed. E-mail: seppelt@chemie.fu-berlin.de.

(1) Santiso, G. Q.; Haegele, G.; Seppelt, K. *Chem. Eur. J.* **2004**, *10*, 4655−4762.
(2) Weinstock, B.; Classen, H. H. *J. Chem. Phys.* **1959**, *31*, 262−263.
(3) Weinstock, B.; Classen, H. H.; Malm, G. *J. Chem. Phys.* **1960**, *32*, 181−185.
(4) Richardson, A. D.; Hedberg, K.; Lucier, G. M. *Inorg. Chem.* **2000**, *39*, 1787−2793.
(5) Wesendrup, R.; Schwerdtfeger, P. *Inorg. Chem.* **2001**, *40*, 3351−3354.
(6) Lee, M.; Kim, H.; Lee, Y. S.; Kim, M. S. *Angew. Chem., Int. Ed. Engl.* **2005**, *44*, 2929−2931.

10.1021/ic052029f CCC: $33.50
Published on Web 03/28/2006

splitting should be much less, so that at a first approximation it can be disregarded. In other words, calculations and experiments on MoF_6, TcF_6, RuF_6, and RhF_6 should be not influenced by this, and small *Jahn−Teller* effects might be detectable. Indeed these hexafluorides are much less well investigated than their third-row counterparts, with the exception of MoF_6.[7] The M−F distances in RuF_6 and RhF_6 have only been determined by EXAFS measurements.[8] The aim of this work is to obtain structural data as precisely as possible for MoF_6, TcF_6, RuF_6, and RhF_6 and to compare them to those for WF_6, ReF_6, OsF_6, IrF_6, and PtF_6. The method chosen is single-crystal X-ray diffractometry. Also an ordered crystal structure of $O_2^+RhF_6^-$ is given and compared with the similar ordered structure of $O_2^+AuF_6^-$.

Experimental Section

Caution: Handling anhydrous HF or compounds that produce HF upon hydrolysis requires eye and skin protection.

Material and Apparatus. Sample handling was performed using Teflon-PFA ((poly)perfluoroether-tetrafluoroethylene) tubes that are sealed at one end and equipped at the other end with a metal valve and thus connectable to a stainless steel vacuum line. HF was dried by several trap-to-trap condensations and stored in a stainless steel tank over BiF_5.

NMR spectra were recorded on a JEOL multinuclear instrument at 400 MHz for ^{1}H. Spectra were recorded relative to $CFCl_3$ (^{19}F) and $PtCl_6^{2-}/H_2O$ (^{195}Pt) as external standards. The UV−vis IR spectra of TcF_6 were recorded on Perkin-Elmer Lambda 9 (3125−58800 cm^{-1}) and Bruker Vektor 22 (4000−200 cm^{-1}) spectrometers as a gaseous samples with approximately 50 mbar pressure in a 10 cm long stainless steel cell equipped with CaF_2 windows (measurment range = 1000−54 000 cm^{-1} (10 μm − 185 nm)).

Radiation Precautions. ^{99}Tc is a weak β^- emitter. Manipulations of ^{99}Tc compounds were performed in a laboratory approved for the handling of such radioactive material.

Preparation of Transition Metal Hexafluorides. MoF_6 and WF_6. MoF_6 and WF_6 were used from laboratory stocks. Crystals were obtained by cooling solutions in n-C_6F_{14}.

TcF_6. TcF_6 was prepared from 50 mg of NH_4^+ TcO_4^- and 100 mL of elemental fluorine at normal conditions in a 150 mL monel autoclave at 600 °C for 1 h; 0.5 mL of anhydrous HF was put into the autoclave before heating. Evaporation of noncondensable gases (F_2, O_2, and N_2) at −196 °C directly from the autoclave was followed by the condensation of the room-temperature volatiles, TcF_6 and HF, into a Teflon PFA tube in a dynamic vacuum. The tube was sealed at both ends. Recrystallization was done by slow cooling from 0 to −78 °C. The yield is assumed to be quantitative. TcF_6 has also been prepared free of HF, using Tc metal and excess F_2 in a monel autoclave at 400 °C.

RuF_6.[9] Elemental Ru powder was kept in a nickel boat in a monel tube and was fluorinated in a stream of 1:7 F_2/Ar at 400−450 °C. Volatiles are condensed into a double U-tube made of Teflon PFA; the first U-tube was cooled to 0 °C, and the second was cooled to −78 °C. Brown deposits condensed in the first trap, and black deposits of RuF_6 were in the second. The Ru powder was consumed completely. The second tube was sealed at one end; HF was condensed in, and the second end was sealed. Recrystallization for O °C to −78 °C yielded black crystals of RuF_6. The isolated yield is below 10%.

RhF_6^-. The older literature procedures of RhF_6 failed totally. The burning of a rhodium wire in a F_2 atmosphere at −196 °C gave no measurable amount, although it has been claimed to be the best method.[10] Bartlett et al. reported yields of only 8% by this procedure.[11] Treatment of Rh powder by F_2/A_2 at 450°,[9] as in the preparation of RuF_6, gave tiny amounts that, with the traces of oxygen present, converted to $O_2^+RhF_6^-$, which recrystallized in the form of red cubes from HF.

The preparation of RhF_6, although in small yields, was achieved by reacting $KAgF_3$, BiF_5, and $KRhF_6$ according to ref 12(the latter is prepared in the sequence $Rh + Cl_2 \xrightarrow{800°} RhCl_3 \xrightarrow[1\ bar]{F_2/400°} RhF_3$ [13] $\xrightarrow[380°C,\ 6\ bar]{F_2} RhF_5$ [14] $\xrightarrow{KF,HF} KRhF_6$). Within a few hours at 0 °C a brown solution was obtained that yielded a very small amount of needle-shaped black RhF_6 crystals upon cooling to −83 °C. The brown insoluble deposits are obviously RhF_5.

ReF_6. ReF_6 was obtained by the literature method[15] of reacting 7 g of ReF_7 (prepared from Re powder and excess F_2 at 400 °C in a monel autoclave overnight) and 0.7 g of Re powder in a monel autoclave at 300 °C).

OsF_6 and IrF_6. OsF_6 and IrF_6 were obtained via the reaction of Os and Ir powders in monel autoclaves at 300 °C. The conversion is quantitative.

PtF_6. PtF_6 was obtained by electrically heating a platinum wire of 0.1 mm diameter in an atmosphere of elemental fluorine in a monel can at −196 °C. The yields based on platinum are usually better than 60%, occasionally even 90%.[12]

$O_2^+AuF_6^-$. $O_2^+AuF_6^-$ was prepared as previously described from O_2, F_2, and Au powders in a monel autoclave at 350 °C.[16,17]

Single crystals were grown from n-C_6F_{14} or HF by slow cooling from 0 to −78° (−83° for RhF_6) over a period of 2−3 days. Crystals were handled with cooling to approximately −140 °C under nitrogen in a special device,[18] and mounted on a Bruker SMART CCD 1000 TU diffractometer using Mo Kα irradiation, a graphite monochromator, a scan width of 0.3° in ω, and a measuring time of 20 s per frame. Each compound was measured up to $2\theta = 85°$ by 3600 frames, thus covering a full sphere. Semiempirical absorption corrections (SADABS) were used by equalizing symmetry-equivalent reflections. Since the refractive power of the compound was high, very small crystals of approximately 0.02 × 0.02 × 0.02 mm were chosen to minimize absorption effects. A needle shaped specimen of 0.05 × 0.02 × 0.01 mm had to be chosen for the extremely reactive and unstable RhF_6, which may explain why the crystallographic criteria of quality are a little less good for this species than they are for all other hexafluorides.

(7) Seip, H. M.; Seip, R. *Acta Chem. Scand.* **1966**, *20*, 2698−2710.
(8) Brisdon, A. K.; Holloway, J. H.; Hope, E. G.; Levason, W.; Ogeden, J. S. *J. Chem. Soc., Dalton Trans.* **1992**, 447−449.
(9) Holloway, J. H.; Hope, E. G.; Stanger, G.; Boyd, D. A. *J. Fluorine Chem.* **1992**, *56*, 77−84.
(10) Chernick, C. L.; Claassen, H. H.; Weinstock, B. *J. Am. Chem. Soc.* **1961**, *83*, 3165−3166.
(11) Bartlett, N. In *Preparative Inorganic Reactions*; Jolly, W. L., Ed.; Interscience: New York, 1965; Vol. 2, pp 301−339.
(12) Botkovitz, P.; Lucier, G. M.; Rao, R. P.; Bartlett, N. *Acta Chim. Slov.* **1999**, *46*, 141−154.
(13) Ruff, O.; Ascher, E. *Z. Anorg. Allg. Chem.* **1929**, *183*, 193-213.
(14) Holloway, J. H.; Rao, P. R.; Bartlett, N. *J. Chem. Soc., Chem. Commun.* **1965**, 306−307.
(15) Malm, J. G.; Selig, H. *J. Inorg. Nucl. Chem.* **1961**, *20*, 189−197.
(16) Bartlett, N.; Leary, K. *Rev. Chim. Miner.* **1976**, *13*, 82−97.
(17) Graudejus, O.; Müller, B. G. *Z. Anorg. Allg. Chem.* **1996**, *622*, 1076−1082.
(18) Schumann, H.; Genthe, W.; Hahn, E.; Hossein, M.-B.; Helm, D. v. d. *J. Organomet. Chem.* **1986**, *28*, 2561−2567.

Table 1. Crystal Data for MF_6 (M = Mo, Tc, Ru, Rh, W, Re, Os, Ir, and Pt)[a]

chemical formula	MoF_6	TcF_6	RuF_6	RhF_6	WF_6	ReF_6	OsF_6	IrF_6	PtF_6
fw	209.94	212.00	215.07	216.91	297.85	297.85	304.2	306.2	309.1
a (pm)	939.4(1)	936.0(3)	931.3(1)	932.3(1)	946.6(1)	941.7(2)	938.7(1)	941.1(1)	937.4(1)
b (pm)	854.3(2)	851.7(3)	848.4(1)	847.4(1)	860.8(1)	857.0(1)	854.3(1)	854.7(1)	852.7(1)
c (pm)	495.9(1)	493.4(2)	491.0(1)	491.0(1)	499.8(1)	496.5(1)	494.4(1)	495.2(1)	493.3(1)
V ($\times 10^6$ pm^3)	397.9(5)	393.3(8)	387.9(3)	387.9(3)	407.2(3)	400.7(4)	396.5(3)	398.3(1)	394.3(1)
μ (mm^{-1})	3.33	3.69	4.07	4.43	28.39	28.86	32.19	33.56	35.61
ρ_{calcd} (g cm^{-1})	3.50	3.58	3.68	3.71	4.86	4.94	5.09	5.11	5.21
R ($I > 4\sigma(I)$	0.015	0.018	0.015	0.026	0.018	0.020	0.021	0.016	0.021
R	0.020	0.020	0.020	0.020	0.020	0.020	0.020	0.013	0.034
wR_2 (all data)	0.031	0.031	0.031	0.031	0.031	0.031	0.031	0.032	0.039

[a] $T = -140$ °C, space group *Pnma*, $Z = 4$, 38 variables, 1540 ± 20 independent reflections.

Structures were solved and refined with the SHELDRICK programs.[19]

All structures refined perfectly in space group *Pnma*; the lower symmetric space group $Pna2_1$ is also possible. The latter has the advantage of having six independent fluorine positions rather than only four (in *Pnma)*, but the results were not as good, and the refinement was less stable. So only the results in *Pnma* are given.

Experimental details of the crystal structure determinations are given in Table 1.

Density functional and ab initio calculations were performed using the GAUSSIAN03 program.[20] The methods B3LYP, B3P86, MP2, and CCSD(T) were used as implemented in the program. The following basis sets were used: 6-31G(d,p) and aug-cc-pVTZ for F. Scalar relativistic energy-consistent pseudopotentials were from the Stuttgart group, [21] and the corresponding basis sets were from Pacific Northwest Laboratory.[22]

Results

The phases of the transition metal hexafluorides have been described long ago. All of them have a cubic high-temperature modification between the melting points and −10 to 3 °C and an orthorhombic low-temperature phase.[23] Neutron powder data on WF_6, OsF_6, and PtF_6 at 5 K gave no indication of further low-temperature modifications,[24] and no additional phases have been observed in any of these hexafluorides in the present study down to −140 °C. Single crystals of good crystallinity have been grown out of C_6F_{14} (WF_6, MoF_6, ReF_6, and OsF_6) and HF solutions (IrF_6, PtF_6, TcF_6, RuF_6, and RhF_6) at temperatures between −30 °C and −83 °C. These crystals have a much better crystallinity than any specimen obtained by sublimation. To achieve highly precise and comparable data, all parameters have been kept constant (e.g., approximate crystal size, the same diffractometer, temperature, 2θ limit, and all other measurement conditions). Results for the second-row transition metal hexafluorides are even better than for their third-row counterparts, since absorption plays a lesser role and the smaller size of the central atoms gives better positional information for the fluorine atoms. In general, the structures could be refined down to conventional *R* values of 2% and often less, and more importantly, the σ values for the bond lengths are only $6-10 \times 10^{-2}$ pm for the second-row hexafluorides and $10-15 \times 10^{-2}$ pm for the third-row hexafluorides. This is a factor of 2 to 3 better than the precise electron-diffraction structural data on third-row hexafluorides.

Table 2. Crystal Data of $O_2^+RhF_6^-$ and $O_2^+AuF_6^-$[a]

chemical formula	O_2RhF_6	O_2AuF_6
fw	124.5	171.8
a (pm)	491.18(5)	496.6(2)
b (pm)	496.43(5)	499.1(2)
c (pm)	497.06(5)	503.5(2)
α (deg)	78.691(3)	101.33(1)[b]
β (deg)	89.656(4)	90.69(1)
γ (deg)	77.806(4)	102.07(1)
V ($\times 10^6$ pm^3)	116.09(2)	119.56(3)
μ (mm^{-1})	3.76	30.87
ρ_{calcd} (g cm^{-1})	3.56	4.77
variables	44	44
independent reflns	1627	1603
R ($I > 4\sigma(I)$	0.013	0.032
R, wR_2 (all data)	0.013, 0.032	0.032, 0.072

[a] Space group $P\bar{1}$, $Z = 1$, $T = -140$ °C. [b] Convention in crystallography enforces these settings. The relationship of the two structures is more evident if, for example, for $O_2^+AuF_6^-$, the unconventional setting $a = 499.1(2)$ pm, $b = 496.6(2)$ pm, $c = 503.5(2)$ pm, $\alpha = 78.67(1)°$, $\beta = 89.31(1)°$, $\gamma = 77.93(1)°$ is chosen.

Experimental conditions are summarized in Table 1, and the results of the single-crystal structure solutions are in Table 2. All compounds crystallize in space group *Pnma*. This results in four different positions for the six fluorine atoms (see Figure 1). There is no indication of any disorder in any of these structures. Lattice parameters, atomic positional parameters, and displacement parameters are very similar. All molecules are very close to or completely octahedral. Angles deviate from the ideal 90° and 180° by not more

(19) Sheldrich, G. *Program for Crystal Structure Solution*; Universität Göttingen: Göttingen, Germany, 1986; *SHELXS*; Universität Göttingen: Göttingen, Germany, 1997.
(20) Frisch, M. J.; Trucks, G. W.; Schlegel, H. B.; Scuseria, G. E.; Robb, M. A.; Cheeseman, J. R.; Montgomery, J. A., Jr.; Vreven, T.; Kudin, K. N.; Burant, J. C.; Millam, J. M.; Iyengar, S. S.; Tomasi, J.; Barone, V.; Mennucci, B.; Cossi, M.; Scalmani, G.; Rega, N.; Petersson, G. A.; Nakatsuji, H.; Hada, M.; Ehara, M.; Toyota, K.; Fukuda, R.; Hasegawa, J.; Ishida, M.; Nakajima, T.; Honda, Y.; Kitao, O.; Nakai, H.; Klene, M.; Li, X.; Knox, J. E.; Hratchian, H. P.; Cross, J. B.; Bakken, V.; Adamo, C.; Jaramillo, J.; Gomperts, R.; Stratmann, R. E.; Yazyev, O.; Austin, A. J.; Cammi, R.; Pomelli, C.; Ochterski, J. W.; Ayala, P. Y.; Morokuma, K.; Voth, G. A.; Salvador, P.; Dannenberg, J. J.; Zakrzewski, V. G.; Dapprich, S.; Daniels, A. D.; Strain, M. C.; Farkas, O.; Malick, D. K.; Rabuck, A. D.; Raghavachari, K.; Foresman, J. B.; Ortiz, J. V.; Cui, Q.; Baboul, A. G.; Clifford, S.; Cioslowski, J.; Stefanov, B. B.; Liu, G.; Liashenko, A.; Piskorz, P.; Komaromi, I.; Martin, R. L.; Fox, D. J.; Keith, T.; Al-Laham, M. A.; Peng, C. Y.; Nanayakkara, A.; Challacombe, M.; Gill, P. M. W.; Johnson, B.; Chen, W.; Wong, M. W.; Gonzalez, C.; Pople, J. A. *Gaussian 03*, revision B.04; Gaussian, Inc.: Pittsburgh, PA, 2003.
(21) Institut fuer Theoretische Chemie, Universität Stuttgart, Stuttgart, Germany.
(22) *Extensive Computational Chemistry Environment Basis Set Database*, version 1.0; Molecular Science Computing Facility, Environment and Molecular Sciences Laboratory, Pacific Northwest Laboratory: Richland, WA; Hay−Wadt ($n + 1$) VDZ effective core potentials.
(23) Siegel, S.; Northrop, D. A. *Inorg. Chem.* **1966**, *5*, 2187−2188.
(24) Marx, R.; Seppelt, K.; Ibbeson, R. M. *J. Chem. Phys.* **1996**, *104*, 7658−7662.

Table 3. Bond Lengths (pm) of MF_6

	M−F1	M−F2 (2×)	M−F3	M−F4 (2×)	ΔM−F[a]	Δ_{max}ang (deg)[b]	*r*(ED)[c]
MoF_6	182.01(8)	181.47(6)	181.59(8)	181.72(6)	0.54	0.25	182.0(3)
TcF_6	181.62(11)	180.94(8)	181.32(11)	181.12(8)	0.68	0.22	
RuF_6	182.24(9)	181.60(6)	181.95(9)	181.61(6)	0.64	0.28	
RhF_6	182.54(16)	182.26(12)	182.24(16)	182.48(11)	0.28	0.25	
WF_6	182.64(18)	182.61(13)	182.66(19)	182.63(12)	0.05	0.44	182.9(2)
ReF_6	182.82(22)	182.06(17)	182.42(22)	182.33(15)	0.76	0.43	182.9(2)
OsF_6	183.33(24)	182.21(18)	182.80(25)	182.92(18)	1.12	0.42	182.8(2)
IrF_6	183.66(18)	183.09(13)	183.47(18)	183.22(13)	0.57	0.25	183.9(2)
PtF_6	184.96(25)	184.90(19)	185.13(27)	184.82(19)	0.31	0.31	185.2(2)

[a] ΔM−F is the largest difference of any measured M−F bond lengths (pm). [b] Δ_{max}ang is the maximal deviation from the 90° and 180° angles of the ideal octahedron. [c] Bond lengths from electron diffraction.[4,25]

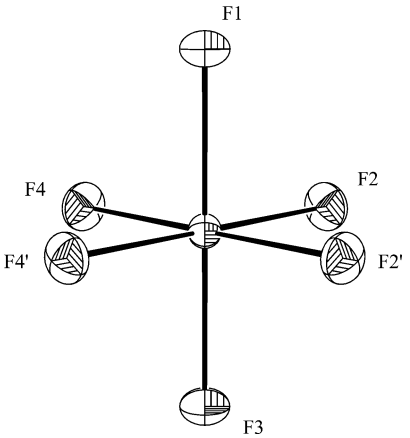

Figure 1. ORTEP diagram of the molecular structure of TcF_6 (50% probability plot).

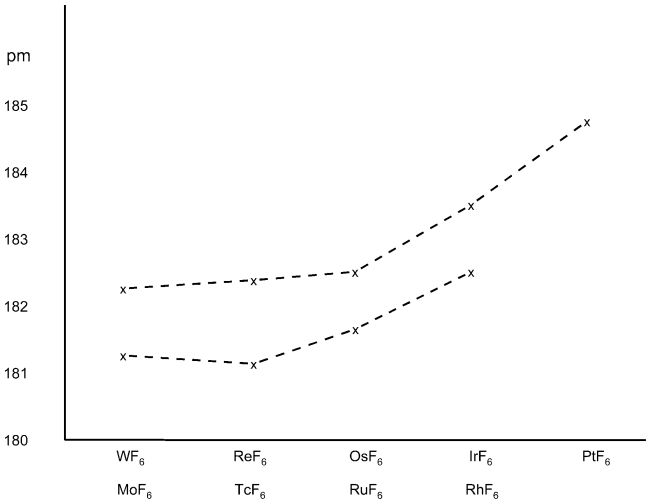

Figure 2. Averaged bond lengths in solid transition metal hexafluorides.

than 0.44°, well within 1σ. Bond lengths within one molecule differ very little (maximum of 5σ), sometimes almost not at all (1σ, WF_6). In Figure 2 the averaged bond lengths are plotted, and the previously established [4,25] trend $r_{W-F} \cong r_{Re-F} \cong r_{Os-F} < r_{Ir-F} < r_{Pt-F}$ is confirmed also for the solid state. A similar trend $r_{Mo-F} \cong r_{Tc-F} \cong r_{Ru-F} < r_{Rh-F}$ is found for the second transition metal series for the first time. The volume per molecule (= 1/4 volume of the unit cell) shows an almost steady decrease.[25] This, in combination with the increasing bond length, is a consequence of the intermolecular F···F distance being decreased, indicating increasing intermolecular forces. The direction and number of the intermolecular F···F contacts are the same in all of these hexafluorides, and therefore they need not to be discussed in detail.

Density Functional and ab initio calculations (see Table 4), have been performed with the spin−orbit coupling being neglected completely. We justify this by showing the wide range absorption spectrum of TcF_6 (Figure 3). The spectra of MoF_6, WF_6, ReF_6, OsF_6, IrF_6, and PtF_6 have been measured before.[26,27] MoF_6 and WF_6 are completely transparent from 1200 to 35 000 (WF_6) and 44 000 cm^{-1} MoF_6.[26] Above these limits, a broad charge-transfer absorption sets in. The spectrum of ReF_6 has been a model for the other 5d hexafluorides and shows, in addition to the charge-transfer absorptions, two additional features at around 5200 cm^{-1} and 32 500 cm^{-1}, both with some vibrational fine structure.[26] The first is assigned to a $t_{3/2} \rightarrow t_{1/2}$ absorption, the splitting of the t_{2g} term being caused by spin−orbit interactions, and a ζ constant of 3500 cm^{-1} is derived from this. The band at 32 500 cm^1 is the $t_{3/2} \rightarrow e_g$ transition, which is caused by the very strong ligand field. As expected, in TcF_6 the low-energy band is completely absent. If a spin−orbit splitting in 4d elements is assumed to be approximately 30% of that in 5d elements,[28] the corresponding absorption would fall into the vibrational region.

On the other hand, in TcF_6, the $t_{2g} \rightarrow e_g$ ligand field transition is clearly observable as a weak band at 31 000 cm^{-1} (see Figure 3), having some vibrational fine structure. The ligand field splitting 10 Dq is thus as high as in ReF_6. Unfortunately, the instability of RuF_6 and RhF_6 did not allow gas UV measurements.

DFT and ab initio calculations (Table 3) predict MoF_6 and RhF_6 to be strictly octahedral, whereas TcF_6 is assumed to be a D_{4h} compressed octahedron; triplet RuF_6 is a D_{4h} elongated octahedron. Singlet RuF_6 is approximately 25 kcal higher in energy but is a D_{4h} compressed octahedron. Similar to the calculations of the third transition row hexafluorides, these distorted octahedral structures are very close in energy

(25) Graudejus, O.; Wilkinson, A. P.; Chacón, L. C.; Bartlett, N. *Inorg. Chem.* **2000**, *39*, 2794−2800.

(26) Moffit, W.; Goodman, G. L.; Fred, M.; Weinstock, B. *Mol. Phys.* **1959**, *2*, 109−122.

(27) Tanner, K. N.; Duncan, A. B. F. *J. Am. Chem. Soc.* **1951**, *73*, 1164−1167.

(28) Gabuda, S. P.; Ikorskii, V. N.; Kozlova, S. G.; Nikitin, P. S. *Pis'ma Zh. Eksp. Teor. Fiz.* **2001**, *73*, 41−44; *JETP Lett. (Engl. Transl.)* **2001**, *73*, 35−38.

Table 4. Calculated Bond Lengths in M−F6 Molecules, Energies, and Adiabatic Electron Affinity

		M−F (pm)	energy (au)
MoF_6 (O_h)	A[a]	186.62	−667.6061637
	B	183.99	−667.7152421
	C	183.50	−667.202192
	D	182.51	−668.4450517
	E	182.40	−666.4994696
electron affinity	C	4.11 eV	
TcF_6 (D_{4h})	A	184.22 (2×)	−680.08218
		186.95 (4×)	
	B	181.07 (2×)	−680.186303
		184.46 (4×)	
	C	181.63 (2×)	−679.4084035
		184.89	
	D	180.54 (2×)	−680.6763083
		183.73 (4×)	
	E	179.72 (2×)	−678.8915486
		184.45 (4×)	
electron affinity	C	5.64 eV	
$TcF_6(O_h)$	A	186.77	−680.08148
	B	181.56	−680.1843398
	C	184.64	−679.407426972
	D	183.49	−680.675308635
	E	182.68	−678.8905636
$RuF_6(D_{4h})$	A	187.64 (2×)	−694.06511
		185.49 (4×)	
	B	185.22 (2×)	−694.1625943
		182.47 (4×)	
	C	185.91 (2×)	−693.1049366
		183.29 (4×)	
	D	184.67 (2×)	−694.3969041
		182.04 (4×)	
	E	183.07 (2×)	−692.7909448
		180.96 (4×)	
	F	182.94 (2×)	−691.7560779
		180.35 (4×)	
electron affinity	C	6.98 eV	
	F	6.98 eV	
RuF_6 (O_h)	A	185.59	−694.06468
	B	182.58	−694.1618329
	C	183.44	−693.104288658
	D	182.18	−694.39621173
	E	181.12	−692.790492
RuF_6 (D_{4h}, sing)	A	183.11 (2×)	−694.02767
		187.99 (4×)	
	B	179.51 (2×)	−694.12456
		185.56 (4×)	
	C	180.59 (2×)	−693.0676299
		186.26 (4×)	
	D	179.34	−694.3587755
		185.01	
	E	179.70 (2×)	−692.7614964
		184.33 (4×)	
$RhF_6(O_h)$	A	186.97	−709.63345
	B	184.30	−709.7227376
	C	184.63	−708.637895
	D	183.27	−709.95289
	E	180.1025	−708.2653904
	F	181.39	−708.275047
electron affinity	C	6.60 eV	
	F	6.44 eV	

[a] A Becke 3LYP, RSC Stuttgart relativistic basis sets, 6−31g(d,p) F basis set; B Becke 3LYP, RSC Stuttgart relativist basis sets, aug-cc-pVT F basis set; C Becke 3LYP, Hay-Wadt ($n + 1$) VDZ effective core potentials, aug-cc-pVT F basis set; D Becke 3P86, Hay-Wadt ($n + 1$) VDZ effective core potentials, aug-cc-pVT F basis set; E MP2, RSC Stuttgart relativistic basis sets, aug-cc-pVT F basis set; F CCSD(T), Hay-Wadt ($n + 1$) VDZ effective core potentials, aug-cc-pVTZ F basis set.

to the regular octahedral transition states (~2.5 kJ mol^{-1}). The calculations have problems with reproducing the experimental bond lengths; only the B3P86 method came close. The other DFT method predict bond lengths too long, and those predicted with MP2 were too short, especially in the case of RhF_6.

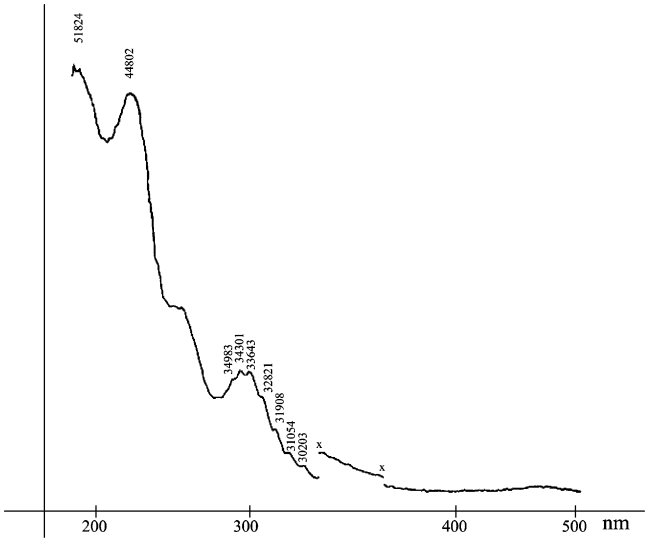

Figure 3. Absorption spectrum of TcF_6 in the UV region. Between 1500 and 20 000 cm^{-1} (6.6 μm and 500 nm), it is completely transparent; x indicates changes in the spectrometer set up. Numerical values in the graph are given per centimeter.

$O_2^+RhF_6^-$ and $O_2^+AuF_6^-$. The difficulties in obtaining highly unstable and reactive RuF_6 and, especially, RhF_6 resulted occasionally in the formation of $O_2^+RuF_6^-$ and $O_2^+RhF_6^-$. The known, expected octahedral structure of $O_2^+RuF_6^-$ with a disordered O_2^+ cation, is confirmed and does not need to be discussed again.[12] $O_2^+RhF_6^-$ appears in a triclinic form if recrystallized from HF at low temperatures. It is isostructural with triclinic $O_2^+AuF_6^-$, whose structure has been published only recently.[29,30] These two structures are free of disorder and have, as their only constraint, a symmetry center at the metal atom. By using crystals as perfect as possible and by applying the same measurement routines as for the MF_6 compounds, we found that AuF_6^- is essentially strictly octahedral.[31] HF, MP2, LDF,[30] MP2, CCSD, and CCSD(T) calculations[32] all arrive at an octahedral structure for AuF_6^-. Experimentally, RhF_6^- shows a fairly strongly compressed octahedron, although the interionic interactions are qualitatively the same as in $O_2^+AuF_6^-$. Without further discussion, we suggest that here a static Jahn−Teller effect on the RhF_6^- (d^4) might be visible. However, we hesitate to draw a final conclusion since this observation is based only on these two crystal structures. Theoretical calculations on RhF_6^- result in bond lengths a few pm too long, but the relative sizes of these values are

(29) Hwang, I.-C.; Seppelt, K. *Angew. Chem., Int. Ed. Engl.* **2001**, *40*, 3690−3692.
(30) Lehmann, J. F.; Schrobilgen, G. J. *J. Fluorine Chem.* **2003**, *119*, 109−124.
(31) Obviously, because of the three very similar lattice constants and two very similar lattice angles, $O_2^+AuF_6^-$ tends to form multiple twinned crystals. This is certainly the reason the two previous structure determinations[23,24] have quite large esd values for the Au−F distance (~1 pm). Here, we present a structure with an esd of 0.3 pm, which still is not as good as the 0.06 pm value in $O_2^+RhF_6^-$.
(32) Seth, M.; Cooke, F.; Schwerdtfeger, P.; Heully, J.-L.; Pelissier, M. *J. Chem. Phys.* **1998**, *109*, 3935−3943.

Table 5. Experimental and Calculated Bond Lengths (pm) of $O_2^+RhF_6^-$ and $O_2^+AuF_6^-$ Triclinic Low Temperature Modifications

	$O_2^+RhF_6^-$							$O_2^+AuF_6^-$
		calcd[a]						
	x-ray	A, D_{4h}	B, D_{4h}	C, D_{4h}	D, D_{4h}	D, O_h	E, D_{4h}	F, D_{4h}	x-ray
O−O	111.07(16)								110.91(28)
M−F_1	186.08(6)	191.18	189.94	190.19	188.72		188.37	182.79	189.98(30)
M−F_2	186.03(6)					188.51			189.87(30)
M−F_3	184.05(7)	188.69	186.28	186.71	185.28		184.60	186.88	189.93(31)
angles (deg)	88.90−91.44(3)	90	90	90	90	90	90	90	88.41−92.71(15)
	180.00	180	180	180	180	180	180	180	180.00
energy (au)		−709.882422	−709.962240	−708.880362	−710.210039	−710.209145	−707.636660	−708.5117208	

[a] A Becke 3LYP, RSC Stuttgart relativistic basis set, 6−31g(d,p) F basis set; B Becke 3LYP, RSC Stuttgart relativist basis set, aug-cc-pVT F basis set; C Becke 3LYP, Hay-Wadt (n + 1) VDZ effective core potentials, aug-cc-pVT F basis set; D Becke 3P86, Hay-Wadt (n + 1) VDZ effective core potentials, aug-cc-pVT F basis set; E MP2, RSC Stuttgart relativistic basis set, aug-cc-pVT F basis set; F CSDC(T), Hay-Wadt (n + 1) VDZ effective core potential, aug-cc-pVTZ F basis set

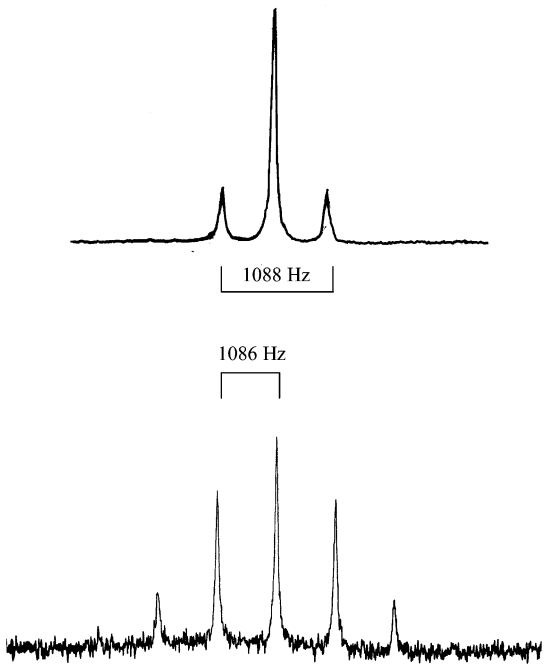

Figure 4. ^{19}F (top) and ^{195}Pt (bottom) NMR spectra of PtF_6 dissolved in n-C_6F_{14}. ^{19}F NMR: δ 3927.7 ppm. ^{195}Pt−NMR: δ −4521.3 ppm (δ $PtCl_6^{2-}$), $J_{19F-195Pt}$ = 1086 Hz.

very closely reproduced (see Table 5). Again the energy difference between the D_{4h} and O_h structures is only 2.5 kJ mol^{-1}.

RhF_6^- has the same valence electron count as PtF_6. In PtF_6, the spin−orbit splitting generates a ground-state $t^4_{3/2}$ with J = O, in other words, a singlet state. This results in a very low temperature-independent paramagnetism[33] and allows the observation of highly resolved ^{19}F and ^{195}Pt NMR spectra in solution (Figure 4) that otherwise would not be observable. The other hexafluorides discussed here have either very broad or nonobservable NMR spectra (except for WF_6 and MoF_6).[34] These findings alone indicate that spin−orbit coupling is very important for the third-row transition metal hexafluorides.

Discussion

All transition metal hexafluorides have very similar crystallographic properties. The decrease of the volume per molecule, already established for the series $WF_6 \rightarrow PtF_6$, is now established also for the series $MoF_6 \rightarrow RhF_6$. Also it is now clear that the last members of these series, IrF_6, PtF_6, and RhF_6 have slightly longer M−F bond lengths in comparison to the other corresponding hexafluorides. Both effects combined mean that the intermolecular F···F contacts will get stronger if one moves from left to right in the periodic system. Parallel to this observation is the decrease in vapor pressure, WF_6 being the most volatile compound and RhF_6 the least. The obvious explanation for these effects is a decrease of the bond polarity in the sequences

$$W \rightarrow \rightarrow \rightarrow Re\ PtF_6 \quad \text{and} \quad MoF_6 \rightarrow \rightarrow \rightarrow RhF_6$$

In no case does the intramolecular bond length vary markedly and certainly not by the margin that the theoretical calculations predict. Therefore we can only support the statement[4,5] that, if there is any distortion present from O_h symmetry, it must be very small. The possibility that bond length deviations might be hidden in the displacement parameters of the fluorine atoms is not obvious, since they are also very much alike in all nine hexafluorides.

It is now well documented, both experimentally and by calculations, that the electron affinity of the third-row transition metal hexafluorides increases stepwise from WF_6 to PtF_6, roughly by 1 eV, to reach the maximum of 6.5−7.0 eV at PtF_6.[5,25] Qualitatively it has been observed that the second-row transition metal hexafluorides obviously have a higher electron affinity. Our calculations, also presented in Table 4, show this indeed. It is interesting to note, however, that RuF_6 has a higher electron affinity than RhF_6. The highest-calculated electron affinity of 6.98 eV for RuF_6 is certainly a result of the stable (octahedral) t^3_{2g} electron configuration of RuF_6^- and is thus essentially as high as the EA of PtF_6. Our calculated electron affinities including those obtained by the coupled-cluster (CSDCT) method are in general more than 1 eV higher than the Xα calculations from 1984 .[35] Experimental values of 7.4 ± 0.3 (PtF_6) and 6.6 ±

(33) Blinc, R.; Pirkmajer, E.; Slivnik, J.; Jupancic, I. *J. Chem. Phys.* **1966**, *45*, 1488−1495.
(34) Seppelt, K.; Bartlett, N. *Z. Anorg. Allg. Chem.* **1977**, *436*, 122−126.
(35) Gutzev, J. L.; Boldyrev, A. I. *Mol. Phys.* **1984**, *53*, 23−31.

0.3 eV (RuF_6) may also have to be remeasured.[36] Also the electron affinity of RhF_6 is close to that of PtF_6. This is in agreement with the chemical reactivity: RuF_6, RhF_6, and PtF_6 oxidize O_2 and Xe.

Acknowledgment. We thank Prof. U. Abram for help with the manipulations of the ^{99}Tc compounds. The authors gratefully acknowledge support from the Deutsche Forschungsgemeinschaft and the Fonds der Chemischen Industrie.

Supporting Information Available: Crystallographic data in CIF format. This material is available free of charge via the Internet at http://pubs.acs.org.

IC052029F

(36) Korolov, M. V.; Kuznetzov, S. V.; Chilingarow, N. S.; Siderov, L. N.; *Dokl. Akad. Nauk.* **1987**, *295*, 131−134.